

引用格式: ZHAO Zhibin, CHENG Cheng, LI Quan, et al. Research on All-solid-state Continuous-wave 228 nm Deep Ultraviolet Laser[J]. Acta Photonica Sinica, 2022, 51(9):0914003

赵志斌,程成,李权,等.全固态连续 228 nm 深紫外激光器研究[J].光子学报,2022,51(9):0914003

全固态连续 228 nm 深紫外激光器研究

赵志斌^{1,2},程成²,李权²,徐东昕²,陈浩²,刘国军²,乔忠良²,王德波²,郑权³,
曲轶²,薄报学¹

(1 长春理工大学 高功率半导体激光国家重点实验室, 长春 130022)

(2 海南师范大学 物理与电子工程学院 海南省激光技术与光电功能材料重点实验室, 海口 571158)

(3 长春新产业光电技术有限公司, 长春 130103)

摘要:采用 V 型腔腔内二倍频和透镜聚焦方式腔外四倍频结构,基于 Nd:YVO₄ 准三能级激光系统 914 nm 基频光级联非线性光学频率变换获得连续波 228 nm 激光输出。在通常情况下,与脉冲运转方式相比,连续运转激光实现透镜聚焦腔外倍频需要较高的平均功率和较好的光束质量。为了获得较高 457 nm 连续激光输出性能,理论计算 V 型腔分臂的长度变化对腔内不同位置光斑大小的影响;实验研究了 V 型腔不同分臂长度对 LD 端泵 Nd:YVO₄/LBO 产生 457 nm 激光输出性能的影响。最终,在泵浦功率为 26 W 时,获得功率为 2.2 W 的 TEM₀₀ 模连续波 457 nm 激光输出,利用 I 类临界相位匹配 BBO 晶体对其进行腔外倍频,获得功率为 6 mW 的 228 nm 连续波深紫外激光,激光光斑呈椭圆形,一小时内功率稳定性为 1.8%。

关键词:激光器;全固态激光器;四倍频;深紫外激光;连续波 228 nm 激光

中图分类号: TN248.1

文献标识码: A

doi:10.3788/gzxb20225109.0914003

0 引言

228 nm 波段在紫外共振拉曼光谱技术中具有非常重要的应用,例如检测 DNA 甲基化^[1]和蛋白质结构^[2-3],此外还可检测炸药^[4]。其原因是,228 nm 谱线激发,可使胞嘧啶(DNA 成分)、氨基酸(蛋白质成分)和 NO_x(炸药成分)中分子的 π 电子系统能级发生跃迁,进而增加拉曼强度^[5]。另外,在灭活细菌病毒方面,在低剂量辐照下,与典型的 254 nm 深紫外线相比,200~230 nm 波段紫外线同样可以灭活细菌、空气中的流感和 SARS-CoV-2 病毒等病原体而几乎不损害人体细胞^[6-9]。国际上把 200~230 nm 波段深紫外光命名为“远紫外线”。2022 年中国冬季奥运会广泛使用远紫外线进行杀菌消毒,并称之为“光疫苗”。与杀菌用典型 254 nm 紫外线相比,远紫外线对人体细胞无害的生物物理原理是蛋白质对该波段存在吸收峰^[10],远紫外线可以穿过比人体细胞小得多的微生物(细菌或病毒典型直径 1 μm 和 0.1 μm)^[11],而典型人体细胞的直径范围约为 10~25 μm ,远紫外线被人体细胞质中的蛋白质强烈吸收,并且在到达人体细胞核之前急剧减弱^[12]。在远紫外线(200~230 nm)波段范围内,准分子灯发射峰值波长为 222 nm 光,且已初步投入使用。激光光源能实现远距离传输,在远距灭菌消毒领域可弥补准分子灯的不足。因此,开展远紫外线(200~230 nm)波段内新型光源的研究具有非常重要的研究意义。

上述采用紫外共振拉曼光谱技术检测生物分子和炸药用的 228 nm 深紫外激光光源,通常使用输出功率

基金项目:海南省重大科技计划(No. ZDKJ2019005),国家自然科学基金(Nos. 61774024, 61864002, 61964007, 11764012),海南省院士创新平台科研专项项目(No. YSPTZX202034),海南省重点研发项目(Nos. ZDYF2020020, ZDYF2020036),海南省自然科学基金(Nos. 519MS051, 121QN228),海南省研究生创新科研课题(Nos. Qhys2021-325, hsyx2021-85)

第一作者:赵志斌(1988—),男,博士研究生,主要研究方向为全固态激光器及非线性光学频率转换技术。Email: 124524871@qq.com

导师:薄报学(1964—),男,教授,博士,主要研究方向为高功率半导体激光器及其应用。Email: 1523001971@qq.com

通讯作者:曲轶(1969—),男,教授,博士,主要研究方向为半导体器件及其应用。Email: 268656673@qq.com

收稿日期:2022-03-30; **录用日期:**2022-05-12

<http://www.photon.ac.cn>

在 mW 量级的 Ti:sapphire 激光器^[2-4],但是 Ti:sapphire 激光器的泵浦源通常采用掺 Nd 激光倍频获得的绿光^[13-15],使激光器整体结构较复杂和较高成本。目前,另一个获得 228 nm 激光最直接且结构简单的办法是采用掺 Nd 增益介质准三能级激光系统 0.91 μm 谱线进行四倍频产生。2020 年,国外报道了 LD 端面泵浦 0.91 μm Nd:GdVO₄ 脉冲运转激光四倍频产生 228 nm 光源^[5]。2021 年,本课题组报道了 LD 端面泵浦 0.91 μm Nd:YVO₄ 激光脉冲运转四倍频 228 nm 激光器^[16]。采用脉冲运转方式,有利于实现非线性光学频率变换和提高效率,但同时也使整个系统复杂和增加成本。本文基于紫外共振拉曼光谱技术检测分子结构和杀菌消毒用的需求,研究系统简单紧凑的连续 228 nm 激光器。根据参考文献,目前关于掺 Nd 增益介质准三能级激光系统 0.9 μm 波段四倍频获得连续波深紫外激光鲜有报道。对于连续运转激光的四倍频,为了提高其倍频效率,通常采用单频激光输出结合环形腔四倍频的方法,但是该方案不仅成本高,而且结构较复杂,不建议使用。本文采用 V 型腔内二倍频和腔外四倍频部分采用透镜聚焦方式的简单结构。该结构中,激光模式匹配、二倍频晶体的摆放位置,以及四倍频部分聚焦镜焦距和四倍频晶体长度的选取是实现连续 228 nm 激光输出的关键因素。本文通过理论研究和实验优化 V 型激光谐振腔参数获得较合适的泵浦光与基频光的模式匹配,以及倍频晶体的合理选取和放置,采用 LBO 晶体,对 LD 端面泵浦 Nd:YVO₄ 的 914 nm 基频光进行腔内二倍频获得最大功率为 2.2 W 的 457 nm 连续激光输出,其光束质量因子 M_x^2 和 M_y^2 分别为 1.16 和 1.11,再通过 BBO 晶体对 457 nm 蓝光进行腔外倍频,获得了功率为 6 mW 的 228 nm 深紫外连续波激光。

1 理论分析

1.1 V 型谐振腔

本实验激光谐振腔采用 V 型谐振腔结构,使基频光分臂获得较好的泵浦光与基频光的模式匹配,同时倍频光分臂中具有较小的光腰,增强 914 nm 基频光产生和提高其倍频效率。考虑 Nd:YVO₄ 晶体产生的热焦距,利用 ABCD 矩阵和稳定腔条件,采用 Matlab 程序计算,得到臂长 L_1 和 L_2 对腔内光斑大小的影响,如图 1 所示。从图 1 可以看出,腔不同位置的光斑大小对 L_1 长度变化不敏感,但是对 L_2 长度变化很敏感。掺 Nd 增益介质的准三能级激光系统,模式匹配对其输出性能影响较大。因此,在实验室过程中,为了获得较好模式匹配,要仔细调节臂 L_2 的长度。此外,从腔内不同位置的光斑大小变化可得知,靠近臂 L_2 的反射镜位置,其光斑较小,因此,二倍频晶体要挨着臂 L_2 的反射镜放置。

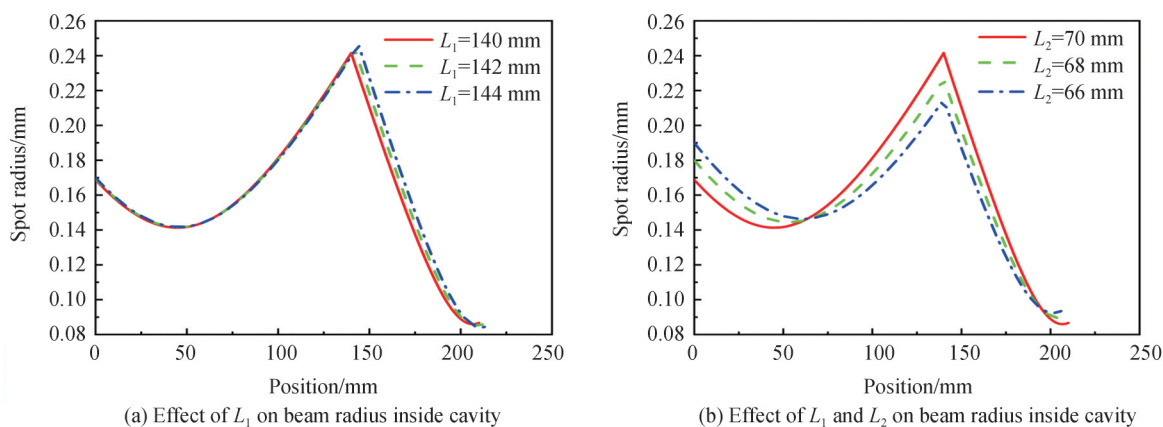


图 1 臂长 L_1 和 L_2 对腔内光斑大小的影响

Fig.1 Effect of L_1 and L_2 on beam radius inside cavity

1.2 倍频晶体的选取

对用与产生 457 nm 蓝光和 228 nm 深紫外光的非线性倍频晶体特性进行总结,如表 1 所示。Lithium triborate LiB₃O₅ (LBO) 和 Bismuth borate BiB₃O₅ (BiBO) 是可以实现近红外波段倍频产生蓝光的两种商业化非线性倍频晶体。在 914 nm 激光二倍频中,虽然 BiBO 具有大的非线性系数 3.44 pm/V,但是其大的走离角 (44.99 mrad),导致获得光斑的光束质量差,因此 BiBO 不适合在本实验中使用。LBO 因具有小的走离角 (12.48 mrad),因此本文选用 LBO 作为二倍频晶体。虽然 LBO 具有小的非线性系数 0.803 pm/V,但是可以

通过延长 LBO 的长度补偿相对较小的非线性系数值。

表 1 可产生 457 nm 与 228 nm 激光的线性晶体特性
Table 1 Nonlinear optical characteristics for 457 nm and 228 nm generation in borate crystals

Crystal		BiBO	LBO	BBO	KBBF	RBBF
Nonlinear coefficient $d_{eff}/(\text{pm}\cdot\text{V}^{-1})$	457 nm	3.44	0.803	2.01	0.436	0.412
	228 nm	—	—	1.38	0.387	0.344
Acceptance angle \times length / (mrad \cdot cm)	457 nm	1.13	4.56	0.89	1.43	1.54
	228 nm	—	—	0.36	0.47	0.52
Walk-off angle / mrad	457 nm	44.99	12.48	61.76	43.36	40.04
	228 nm	—	—	75.68	66.05	58.72
Phase-matching angle / ($^{\circ}$)	457 nm	$\theta=159.6$	$\theta=90.0$	$\theta=25.8$	$\theta=22.0$	$\theta=23.7$
		$\varphi=90.0$	$\varphi=21.7$			
	228nm	—	—	$\theta=61.4$	$\theta=43.9$	$\theta=48.1$
Hygroscopicity		Difficult	Non	Slight	Non	Non
Transmission band range/nm		286~2 500	160~2 600	185~2 600	147~3 500	165~3 500

目前,常用的紫外四倍频非线性晶体主要是 β -BaB₂O₄(BBO)和(CsLiB₆O₁₀)CLBO 晶体。其中,CLBO 晶体具有较高的非线性系数、较小的走离角度以及对紫外波段的激光没有吸收作用等优点,有利于获得较高输出功率、较好光束质量的紫外光输出,但 CLBO 晶体在 457 nm 不能实现相位匹配(对于二倍频)。RbBe₂BO₃F₂ (RBBF)和KBe₂BO₃F₂ (KBBF)晶体也能用于产生紫外光,但是其有效非线性系数较小,而且生产技术还不够成熟,还没有实现稳定的商业化商品,不利于获得较高功率的紫外激光输出。相比于其他晶体,BBO 晶体是较为成熟的一种非线性晶体,具有较大的有效非线性系数及较高的损伤阈值,且光学性能稳定、透光波长范围较宽,是目前用来产生紫外及深紫外波段激光最广泛的一种晶体,并且其生产技术比较成熟。因此,本文选用 BBO 作为四倍频晶体。

2 实验装置

实验装置如图 2 所示。泵浦源采用光纤耦合输出的 LD,其最大输出功率为 110 W,中心波长为 808 nm,光纤芯径是 400 μm ,数值孔径 $\text{NA}=0.22$ 。泵浦光耦合系统由两个焦距 $f=10$ mm 的平凸镜和一个 45° 偏片构成,其成像放大倍数接近 1:1。Nd:YVO₄晶体的尺寸为 $4\times 4\times 5$ mm³,掺杂原子数分数为 0.1%。Nd:YVO₄晶体左端面作为谐振腔的一个端镜 M1,镀有 808 nm、1 064 nm 增透膜和 914 nm 高反膜;晶体的右端面镀有 914 nm、1 064 nm 和 1 342 nm 增透膜。使用 0.1 mm 厚的银箔包裹 Nd:YVO₄晶体侧面,并放置在紫铜热沉中,通过水冷进行温度控制。输出镜 M 是平凹镜,其曲率半径为 100 mm,镀有 914 nm 高反膜,457 nm、1 064 nm 和 1 342 nm 增透膜;平凹镜 M2 作为反射镜,其曲率半径为 200 mm,镀有 457 nm 和 914 nm 高反膜。

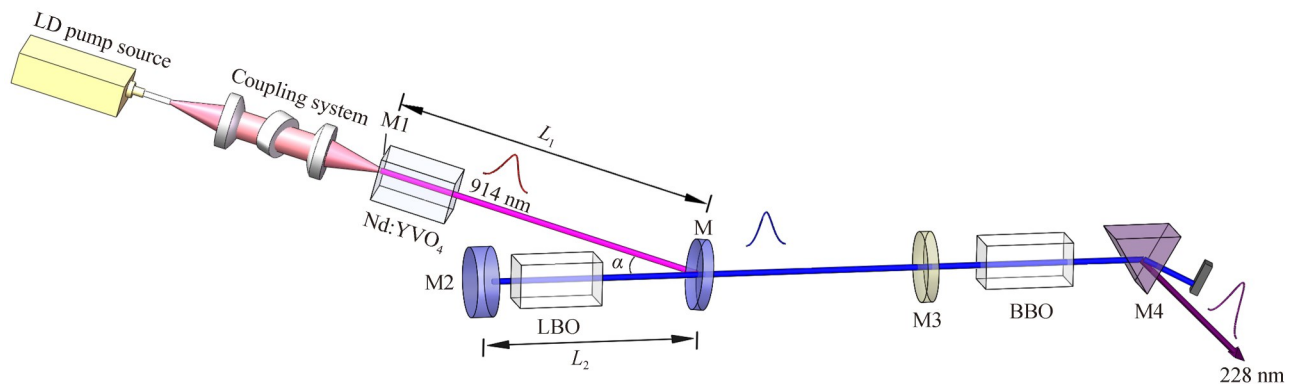


图 2 实验装置
Fig.2 Experimental setup

由Nd:YVO₄晶体的左端面M1、M和M2构成一个V型激光谐振腔,两臂夹角 α 为5°。LBO倍频晶体采用I类临界相位匹配,其切割角度为 $\theta=90^\circ$, $\varphi=21.7^\circ$,尺寸为 $4\times 4\times 15\text{ mm}^3$,晶体两端面镀有457 nm、914 nm和1 064 nm增透膜。M3为457 nm聚焦镜,其焦距为150 mm,镀有457 nm增透膜。BBO倍频晶体的尺寸为 $4\times 4\times 10\text{ mm}^3$,采用I类临界相位匹配,其切割角为 $\theta=61.4^\circ$ 。457 nm激光从镜M输出,经过M3聚焦镜聚焦,在焦点处放置BBO晶体,经过BBO晶体倍频获得228 nm连续深紫外激光。分光棱镜M4用于分离457 nm和228 nm激光。本文的激光光谱采用美国OCEAN OPTICS公司HR4000CG-UV-NIR光谱仪测量,激光输出功率采用以色列OPHIR公司NOVAII和加拿大GENTEC-EO公司MAESTRO激光功率计测量,采用美国THORLABS公司BP209/VIS光束质量分析仪测量激光光斑。

3 457 nm 连续激光输出

基于本实验采用透镜聚焦方式进行腔外四倍频,457 nm连续激光的输出功率和光束质量是产生连续228 nm激光的关键因素。为了获得较高性能的457 nm激光输出,实验中在 $L_1=140\text{ mm}$ 下, L_2 分别取70 mm、68 mm和66 mm,得到457 nm激光输出功率随注入泵浦功率的变化关系如图3(a)所示。在注入泵浦功率为26 W下,获得连续457 nm激光输出的最大功率分别为1.6 W($L_2=70\text{ mm}$)、2.2 W($L_2=68\text{ mm}$)和1.2 W($L_2=66\text{ mm}$),且 $L_2=68\text{ mm}$ 时获得的光斑光束质量比 $L_2=70\text{ mm}$ 和66 mm的好。图3(b)是 $L_2=68\text{ mm}$,在457 nm激光最高输出功率下的光斑和光束质量,得到其光斑为TEM₀₀模。相比 $L_2=70\text{ mm}$ 和66 mm,在 L_2 取68 mm时,获得457 nm激光的输出性能最高,原因是获得较合适的泵浦光与基频光的模式匹配。因此,选取 $L_2=68\text{ mm}$ 的谐振腔产生的457 nm激光进行腔外四倍频。

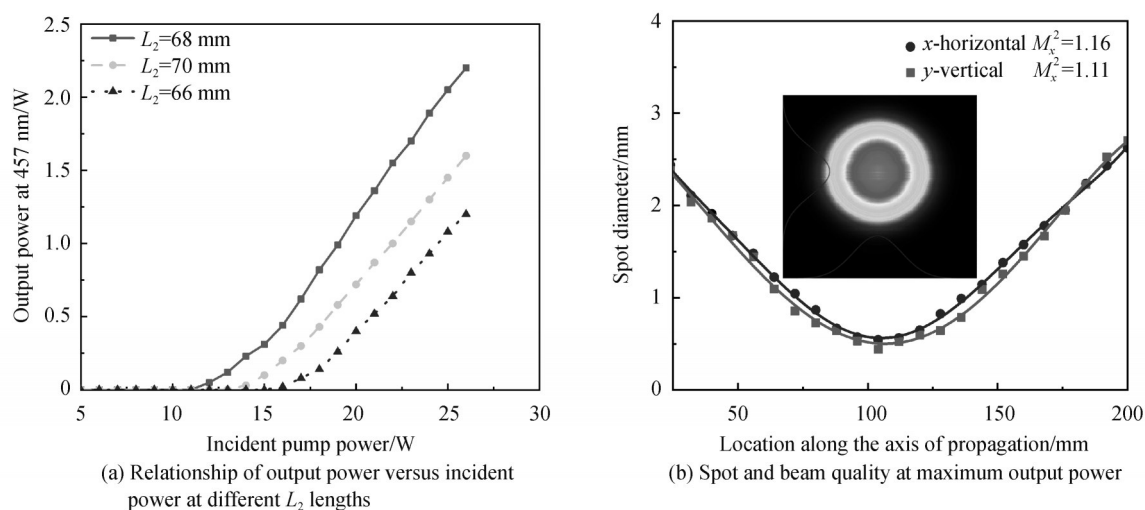


图3 457 nm激光输出特性
Fig.3 Output characteristics of 457 nm laser

4 228 nm 连续激光输出

为了提高457 nm激光的倍频效率,最佳聚焦条件有^[17]

$$\xi = \frac{L}{2Z_r} = 2.84 \quad (1)$$

式中, L 为非线性晶体长度, Z_r 为聚焦光束的瑞利长度。根据式(2),选择合适的位置放置M3聚焦镜和BBO晶体。最终,通过测量得到其光斑大小约为100 μm 。功率为2.2 W的457 nm连续激光经过BBO晶体后,得到功率为6 mW的228 nm深紫外激光。图4(a)深紫外激光输出光谱,峰值在228 nm附近。228 nm激光输出功率与457 nm激光注入功率的关系如图4(b)所示,228 nm激光输出功率随着注入功率增加而增加。图4(c)是228 nm激光光斑,其中右上角是激光照射在白纸上的发光效果,输出光斑为椭圆形,原因是457 nm激光经BBO晶体倍频后,228 nm倍频光的走离角较大。图4(d)为一小时内228 nm激光输出功率在6 mW时

的稳定性测试,得到其稳定度为 1.8%。

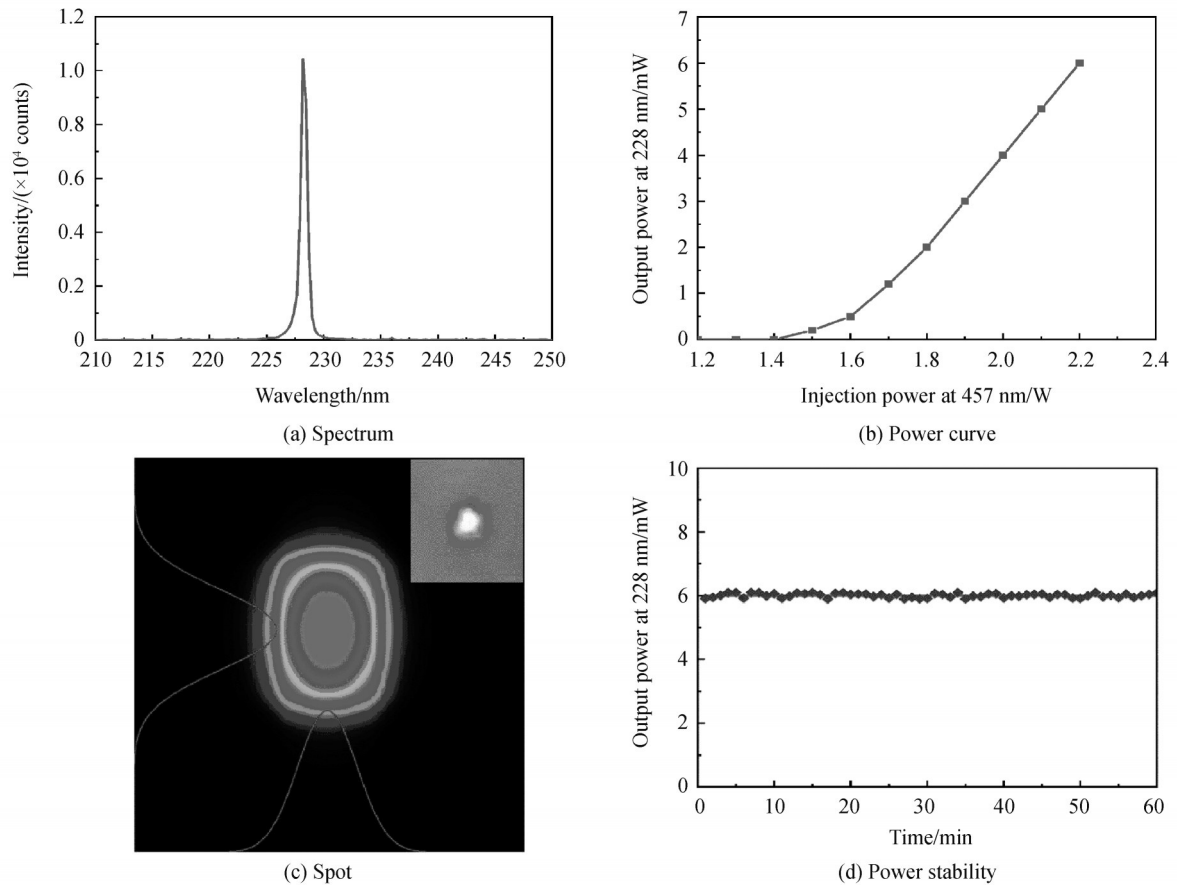


图4 228 nm 连续深紫外激光输出特性

Fig.4 Output characteristics of 228 nm CW DUV laser

5 结论

本文采用V型腔内二倍频和透镜聚焦方式腔外四倍频的结构,基于Nd:YVO₄准三能级激光系统914 nm基频光级联非线性光学频率变换获得全固态连续运转228 nm深紫外激光器。用LD端面泵浦Nd:YVO₄晶体,通过理论研究和实验优化V型激光谐振腔参数获得较合适的泵浦光与基频光的模式匹配,以及倍频晶体的合理选取和放置,采用LBO晶体,对LD端面泵浦Nd:YVO₄的914 nm基频光进行腔内二倍频获得最大功率为2.2 W的457 nm连续激光输出,其光束质量因子 M_x^2 和 M_y^2 分别为1.16和1.11,再通过BBO晶体对457 nm蓝光进行腔外倍频,获得了功率为6 mW的228 nm深紫外连续波激光,激光光斑呈椭圆形,一小时内其功率稳定性为1.8%。该激光器输出性能基本满足紫外共振拉曼光谱技术检测生物分子和杀菌消毒的要求。

参考文献

- [1] D'AMICO F, ZUCCHIATTI P, LATELLA K, et al. Investigation of genomic DNA methylation by ultraviolet resonant Raman spectroscopy[J]. Journal of Biophotonics, 2020, 13(12): e202000150.
- [2] ASAMOTO D A K, KIM J E. UV resonance Raman spectroscopy as a tool to probe membrane protein structure and dynamics[M]. Lipid-Protein Interactions, Humana, New York, 2019: 327-349.
- [3] SHAFAT H S, SANCHEZ K M, NEARY T J, et al. Ultraviolet resonance Raman spectroscopy of a β -sheet peptide: a model for membrane protein folding[J]. Journal of Raman Spectroscopy, 2009, 40(8): 1060-1064.
- [4] LEIGH B S, MONSON K L, KIM J E. Visible and UV resonance Raman spectroscopy of the peroxide-based explosive HMTD and its photoproducts[J]. Forensic Chemistry, 2016, 2: 22-28.
- [5] BYKOV S V, ROPPEL R D, MAO M, et al. 228-nm quadrupled quasi-three-level Nd:GdVO₄ laser for ultraviolet resonance Raman spectroscopy of explosives and biological molecules[J]. Journal of Raman Spectroscopy, 2020, 51(12):

- 2478-2488.
- [6] SOSNIN E A, STOFFELS E, EROFEEV M V, et al. The effects of UV irradiation and gas plasma treatment on living mammalian cells and bacteria: a comparative approach[J]. *IEEE Transactions on Plasma Science*, 2004, 32(4): 1544-1550.
- [7] BUONANNO M, STANISLAUSKAS M, PONNAIYA B, et al. 207-nm UV light—a promising tool for safe low-cost reduction of surgical site infections. II: In-vivo safety studies[J]. *PLoS One*, 2016, 11(6): e0138418.
- [8] WELCH D, BUONANNO M, GRILJ V, et al. Far-UVC light: A new tool to control the spread of airborne-mediated microbial diseases[J]. *Scientific Reports*, 2018, 8(1): 1-7.
- [9] BUONANNO M, WELCH D, SHURYAK I, et al. Far-UVC light (222nm) efficiently and safely inactivates airborne human coronaviruses[J]. *Scientific Reports*, 2020, 10(1):1-8.
- [10] HESSLING M, HAAG R, SIEBER N, et al. The impact of far-UVC radiation (200-230 nm) on pathogens, cells, skin, and eyes - a collection and analysis of a hundred years of data[J]. *GMS Hygiene and Infection Control*, 2021, 16: Doc07.
- [11] METZLER D E. *Biochemistry: The chemical reactions of living cells*[M]. 2nd. San Diego: Academic Press, 2001.
- [12] PFEIFER G P, BESARATINIA A. UV wavelength-dependent DNA damage and human non-melanoma and melanoma skin cancer[J]. *Photochemical & Photobiological Sciences*, 2012, 11(1): 90-97.
- [13] SANCHEZ K M, NEARY T J, KIM J E. Ultraviolet resonance Raman spectroscopy of folded and unfolded states of an integral membrane protein[J]. *The Journal of Physical Chemistry B*, 2008, 112(31): 9507-9511.
- [14] BYKOV S, LEDBEV I, IANOUL A, et al. Steady-state and transient ultraviolet resonance Raman spectrometer for the 193-270 nm spectral region[J]. *Applied Spectroscopy*, 2005, 59(12): 1541-1552.
- [15] ZHAO Shanghong, CHEN Guofu, ZHAO Wei, et al. All-solid-state multi-wavelength laser system from 208 to 830 nm[J]. *Chinese Physics Letters*, 2001, 18(4): 537.
- [16] ZHAO Zhibin, CHEN Hao, LIU Guojun, et al. All-solid-state DUV light source by quadrupling of an acousto-optically Q-switched Nd: YVO₄ Laser[J]. *IEEE Access*, 2021, 9: 165989-165995.
- [17] BOYD G D, KLEINMAN D A. Parametric interaction of focused Gaussian light beams[J]. *Journal of Applied Physics*, 1968, 39(8): 3597-3639.

Research on All-solid-state Continuous-wave 228 nm Deep Ultraviolet Laser

ZHAO Zhibin^{1,2}, CHENG Cheng², LI Quan², XU Dongxin², CHEN Hao², LIU Guojun²,
QIAO Zhongliang², WANG Debo², ZHENG Quan³, QU Yi², BO Baoxue¹

(1 *State Key Laboratory of High Power Semiconductor Laser, Changchun University of Science and Technology, Changchun 130022, China*)

(2 *College of Physics and Electronic Engineering, Key Laboratory of Laser Technology and Optoelectronic Functional Materials of Hainan Province, Hainan Normal University, Haikou 571158, China*)

(3 *Changchun New Industries Optoelectronics Technology Co., Ltd., Changchun 130103, China*)

Abstract: Deep UV laser has very important applications in sterilization, Raman spectroscopy and material processing. In this study, the 914 nm fundamental frequency optical cascade nonlinear optical frequency conversion was realized by the frequency doubling in the V-shaped cavity and Lens focusing method, extra-cavity quadruple frequency structure, 228 nm CW laser was obtained. In general, higher average power and better beam quality were required for the continuous operation laser to achieve the extra-cavity frequency doubling compared with the pulse operation. In order to obtain a higher output performance of 457 nm CW laser, this paper firstly analyzes the influence of the length change of the V-shaped cavity arm on the spot size at different positions in the cavity by theoretical calculation. The effects of different arm lengths of V-cavity on the output performance of 457 nm laser generated by LD end pump Nd: YVO₄/LBO was investigated experimentally. Finally, at pump power of 26 W, 457 nm CW laser output of 2.2 W, TEM₀₀, has been achieved. On the basis of frequency doubling, extra-cavity frequency doubling using Type-I phase matching BBO crystal, was performed, and 228 nm CW DUV laser with 6 mW power has been achieved, the laser spot was elliptic and the power stability was 1.8% within one hour. The pump source is an 808 nm fiber-coupled LD with a core diameter of 400 μm and a numerical aperture of 0.22,

with maximum CW power of 110 W. The pump light coupling system consists of two plano-convex mirrors with a focal length of 10 mm and a 45° polarizer, and its imaging magnification is close to 1:1. The parameters of Nd:YVO₄ crystal are: Nd³⁺ atomic doping concentration is 0.1%; 4×4×5 mm³ in size; the left facet was antireflection coated at 808 nm and 1 064 nm and high reflection coated at 914 nm; the right facet was antireflection coated at 914 nm, 1 064 nm and 1 342 nm wavelengths. The laser crystal was wrapped in a layer of indium foil on the side and secured on a copper heat sink, which is capable of controlling the temperature through circulating water cooling. The output mirror M is a flat concave mirror with a curvature radius of 100 mm. It is coated with 914 nm high reflection film, 457 nm, 1 064 nm and 1 342 nm antireflection film. The high reflection mirror M2 was a flat concave mirror with 200 mm in radius of curvature which was high reflection coated at 457 nm and 914 nm. The V-shape cavity was formed by the left facet of Nd:YVO₄ crystal M1 and M and M2, where the angle between the two arms is 5°. The size of LBO frequency doubling crystal is 4×4×15 mm³, both facets of which were antireflection coated at 457 nm, 914 nm and 1 064 nm. M3 is a 457 nm focusing lens with a focal length of 150 mm and coated with 457 nm antireflective film. The size of BBO frequency doubling crystal is 4×4×8 mm³, and the Type-I phase matching was adopted, the cutting angle is $\theta=61.4^\circ$. The 457 nm laser is output from mirror M and focused through M3 focusing lens, BBO crystal is placed at the focus, and 228 nm CW deep UV laser was obtained by frequency doubling of BBO crystal. The splitting prism M4 was used to separate 457 nm and 228 nm lasers. Considering the thermal focal length generated by Nd:YVO₄ crystal, ABCD matrix and stable cavity conditions were used to calculate by Matlab program, and the influence of arm length L1 and L2 on the size of light spot in the cavity was obtained. As can be seen spot size at different positions of the cavity is insensitive to L1 length change, but sensitive to L2 length change. The L2 length of the V-cavity was optimized experimentally to obtain a more appropriate mode matching between the pump light and the fundamental frequency light. The maximum output power of 457 nm CW laser was 2.2 W and the light spot was TEM₀₀ mode when the pump power was 26 W. Finally, 457 nm CW laser with output power of 2.2 W passes through the BBO crystal to produce 228 nm deep UV laser with 6 mW power. The relationship between the output power of 228 nm laser and the injected power of 457 nm laser is shown, and the stability is 1.8%.

Key words: Laser; All-solid-state laser; Quadruple frequency; Deep ultraviolet laser; Continuous-wave 228 nm laser

OCIS Codes: 140.3460; 140.3580; 140.3515; 140.3610; 350.7420